Hindawi
Mobile Information Systems
Volume 2021, Article ID 9955988, 8 pages
https://doi.org/10.1155/2021/9955988

Research Article

Fatigue Load Spectrum of Highway Bridge Vehicles in Plateau Mountainous Area Based on Wireless Sensing

Li Rui, Xie Xiaoyu, and Duan Xueyan

The Faculty of Civil Engineering and Mechanics, KunMing University of Science and Technology, Kunming 650500, China

Correspondence should be addressed to Li Rui; liruiking@kust.edu.cn

Received 4 March 2021; Revised 30 March 2021; Accepted 15 April 2021; Published 26 April 2021

Academic Editor: Muhammad Usman

In Yunnan and other plateau mountainous areas, hydropower and mineral resources are abundant, and there are relatively many vehicles used for the transportation of large hydropower facilities. The widespread phenomenon of vehicle overload causes severe fatigue among the drivers. However, there is no reference vehicle load spectrum for fatigue analysis in the existing research. The application of wireless sensing technology to bridge health monitoring is favorable for the entire monitoring system's low-cost and intelligent development. In this study, wireless sensors are used to collect sensing data in the measured area and perform preliminary filtering processing. The data collected by the sensing layer is aggregated at the TD gateway layer to realize local short-term storage of monitoring data, and 3G wireless transmission is used for the effective processing of the data. The clustering method is used to classify the vehicle models based on investigating the most representative expressway traffic flow information in Yunnan Province. Moreover, the weighted probability distribution model of different vehicle models is established through statistical analysis, which simplifies the composition's fatigue intensity spectrum model. The selection of five vehicles of the equivalent model followed by a six-axle vehicle has the most significant impact on bridge damage as the standard fatigue vehicle. The research results establish a basis for the fatigue design of highway bridges in plateau and mountainous areas and provide data to establish vehicle fatigue load spectra in national highway regions.

1. Introduction

In recent decades, with the rapid growth of China's economy, quantity and weight of road traffic vehicles grow with each passing day. Bridge accidents caused by fatigue damage of vehicles increase year by year, and fatigue problem attracts more and more attention of the public. Because moving traffic is the major fatigue load for bridge structure, proper selection of fatigue load spectrum of vehicle is the key to rational prediction of fatigue life of bridge structures.

There is fatigue load spectrum of vehicle or standard fatigue vehicle model available for fatigue analysis a long time ago in foreign countries, for example, Specification for Fatigue Implementation, part 10 of BS5400 Bridge Criterion [1] issued by United Kingdom in 1978. This model formulates load frequency spectrum applicable to highway steel bridges in England in the view of statistical data of vehicles on truck highway bridges. AASHTO Load and Resistance Factor Design (LRFD) formulates the first edition of steel bridge fatigue specification on basis of Goodman diagram of American Welding Society and standard fatigue vehicle model applicable to American highway bridges is raised in the specification [2]. The six-axle vehicle weighing 445 kilo newton (kN) in total is selected as standard fatigue vehicle for making fatigue design is raised in General Code for Design of Highway Bridges and Culverts (JTG D60—2015) [3] in China. At the same time, many scholars in China conduct studies on fatigue load spectrum of vehicle. Wang et al. carried out an investigation and studied traffic volume of Hengfu road section on the inner-ring road in Guangzhou City and build fatigue-loaded vehicle model for viaducts in Guangzhou City. Su et al. carried out an investigation and statistical analysis on traffic volume of outer-ring road in Tianjin City and work out fatigue load spectrum applicable to highway bridges in Tianjin City. Le et al. took the bridge on a certain road section in Shanghai City as object of study to conduct a statistical analysis through investigation into vehicular traffic at site and formulate fatigue load spectrum

for fatigue design of road bridges in Shanghai City. Shao et al.'s research results provide anti-fatigue design of bridges and evaluation of fatigue life with reliable vehicle load spectrum on basis of investigation into vehicle load at the site of Jiujiang Yangtze River Bridge [4]. Jiang et al. took Aizhai Bridge on Jicha Highway as engineering background and conducted a random load investigation and study to obtain the load spectrum of random vehicle on Aizhai Bridge [5]. Wang et al. established fatigue load spectrum of beam bridges in road freight passage with mass flow and heavy load. However due to China's vast territory, economic development varies from region to region and traffic operation conditions of all regions are quite different. Fatigue load spectrum obtained from results of investigation into different regions does not have general applicability. Thus, plateau mountainous areas such as Yunnan Province cannot directly apply the fatigue load spectrums of other regions. Specific regional traffic situation shall be combined to formulate the vehicle fatigue load spectrum with regional representativeness [6].

In order to establish the load spectrum of fatigue vehicles on the highway, the major contributions of this work are as follows:

Conducting an investigation into traffic flow information of G56 highway (Kunming to Baoshan road section on Hangzhou-Ruili Highway), and obtaining random distribution characteristic of traffic flow by statistical analysis.

Secondly, a T-beam bridge with a span of 30 meters, which is the most representative bridge type on highway of Yunnan Province, is adopted for fatigue life analysis.

Finally, the load spectrum of fatigue vehicles is established through the principle of equivalence. Meanwhile, a six-axle truck with maximum contribution to fatigue damage was determined as the fatigue standard vehicle model for simplified fatigue analysis [7].

2. Traffic Investigation and Statistics

In this work, wireless sensors network (WSN) is used to accumulate traffic flow data. WSN is a group of dedicated wireless sensors for monitoring and recording the physical conditions of the environment and organizing the collected data at a central location. WSNs measure environmental conditions like temperature,, humidity, wind, and so on. WSN is similar to wireless ad hoc networks in the sense that they rely on wireless connectivity. WSNs are spatially distributed autonomous sensors that cooperatively pass their data through the network to a main location [8].

In virtue of dynamic weighing wireless network sensing system on G56 highway (Kunming to Baoshan road section), observation of vehicular traffic on January 1, 2015, has been made for 24 hours to obtain traffic flow data of 9440 automobiles. Data information includes traffic flow, vehicle model, and weight. In general, all-day traffic flow information obeys a certain rule. Traffic flow has gradually risen from 4 o'clock in the morning and reaches the first peak at 11 o'clock in the morning. Traffic flow falls slightly after lunchtime but begins to recover at about 14 o'clock at noon. It reaches the second peak until 18 o'clock in the afternoon. Numerical values of two peaks have no big gap, about 600 vehicles. Night falls after the second peak and traffic flow falls gradually and then reaches the minimum value at 3 o'clock in the morning of the next day [9].

With reference to automotive models [10] and in view of parameters including number of axles, number of wheels, wheelbase, and vehicle weight, statistics of vehicular traffic data, statistics finds that there are mainly 26 vehicle models. Afterwards, vehicles are classified into 5 typical vehicle models by clustering methodology [11]. Clustering indexes, respectively, select number of axles, number of wheels, overall volume, gross weight, damage coefficient, minimum ground clearance, and vehicle conversion factor. Classification result is shown in Table 1.

In Table 1, there are 6087 type 1 vehicles taking up 64.5% of total vehicles; there are 501 type 2 vehicles taking up 5.3% of total vehicles; there are 1516 type 3 vehicles taking up 16.1% of total vehicles; there are 107 type 4 vehicles taking up 1.1% of total vehicles; there are 1227 type 5 vehicles taking up 13% of total vehicles.

3. Fatigue-Loaded Vehicle Model

3.1. Proportion of Vehicle Models. In order to make proportions of traffic flow more practical in simulative environment, statistical results are computed as shown in Table 2. The idea was based on statistical number of vehicles in each model and exclusion from small vehicles (weighing 3 tons on experience) [6] as with relatively little fatigue damage to bridges. Percent in the bracket represents the proportion of that vehicle model to total number of traffic flow. Proportion of gross vehicles is included in the classification and is 86.4%.

3.2. Vehicle Weight. Random distribution of vehicle weight data of traffic flow has several patterns including normal distribution, logarithmic normal distribution, Weibull distribution, Gamma distribution, and Gaussian mixture distribution. This text, respectively, assumes that vehicle weight data obeys the above-mentioned five distribution patterns. In addition, it utilizes maximum like parameter estimation method such as likelihood method or other approximate formulas to estimate relative parameters of each distribution. It also makes distribution fit tests of all distribution according to Kolmogorov-Smirnov test-related theory in hypothesis testing to find the suitable distribution pattern and to obtain the probability density function of vehicle weight distribution for each vehicle model at last. The Kolmogorov-Smirnov (K-S) test [12] is used to decide if a sample comes from a population with a specific distribution. The K-S test is based on the empirical distribution function (ECDF). Statistical analysis on vehicle weight data is made to obtain the distribution pattern and its probability distribution parameters for each vehicle model in random traffic flow. Please check specific numerical values in Table 3. πi, μi,

Table 1: Classification of typical vehicles.

Vehicle model	Model car	Number of axles	Wheelbase (m)	Axle weight (kN)	Total weight (kN)	Proportion in classification (%)
Type 1	V1–V4	2	—	—	≤30	76
	V5–V7	2	3.3	22, 53	75	6
	V10–V15	2	4.7	40, 60	100	17.9
Type 2	V8-V9	3	4.65, 1.25	50, 64, 64	178	68.4
	V16–V17	3	3.55, 1.32	45, 54, 55	154	6
	V18-V19	3	4.325, 1.35	24, 72, 71	167	25.4
Type 3	V20	4	3.3, 6, 1.35	53, 60, 67, 67	247	69.2
	V21	4	3.4, 7.6, 3	60, 80, 70, 70	280	30.7
Type 4	V22-V23	5	3, 1.35, 7, 1.3	51, 85, 85, 63, 63	347	53.7
	V24	5	3.3, 1.32, 6, 1.35	60, 105, 73, 73, 73	384	47.2
Type 5	V25	6	3.3, 1.32, 6, 1.3, 1.3	51, 85, 85, 79, 79, 79	458	0.4
	V26	6	3.3, 1.32, 6, 1.3, 1.3	45, 65, 90, 67, 60, 60	387	99.5

Table 2: Proportion of various fatigue-loaded vehicle models.

	Type 1	Type 2	Type 3	Type 4	Type 5
Proportion					
	M1: (50.9%)	M2: (5.32%)	M3: (16.07%)	M4: (1.13%)	M5: (13%)

Table 3: Weight distribution of various models of vehicles.

Vehicle model	Distribution pattern	Weight			Distribution parameter I			Distribution parameter II		
Type 1	Lognormal				μ:1.56			σ:0.80		
Type 2	Triple-normal	π_1: 0.50	π_2: 0.46	π_3: 0.04	μ_1: 14.14	μ_2: 24.78	μ_3: 68.85	σ_1: 6.09	σ_2: 18.17	σ_3: 10.73
Type 3	Triple-normal	π_1: 0.49	π_2: 0.46	π_3: 0.05	μ_1: 16.61	μ_2: 38.22	μ_3: 74.88	σ_1: 5.82	σ_2: 15.98	σ_3: 4.27
Type 4	Triple-normal	π_1: 0.32	π_2: 0.39	π_3: 0.29	μ_1: 16.63	μ_2: 39.05	μ_3: 47.69	σ_1: 4.54	σ_2: 7.74	σ_3: 34.79
Type 5	Triple-normal	π_1: 0.22	π_2: 0.31	π_3: 0.47	μ_1: 17.88	μ_2: 39.3	μ_3: 51.47	σ_1: 3.83	σ_2: 10.39	σ_3: 14.05

and σi in the table represent weight function, mean value, and variance at No. i peak, respectively. Shown in Table 3, except type 1 vehicle model obeying logarithmic normal distribution, the remaining four types of vehicle models obey mixed normal distribution.

3.3. Wheelbase. Wheelbase data is obtained by measuring samples of the above types of vehicle models obtained from on-site traffic investigations. The mean value and standard deviation (in bracket) of wheelbases of different vehicle models are shown in Table 4. Axle 1 represents the distance from the second vehicle axle to the first vehicle axle in the direction from vehicle head to tail. The rest of the data is in a similar fashion.

3.4. Axle Weight. According to Chen's study, axle weight has linear approximate relationship [13] with vehicle weight.

$$w_i = a_i W + b_i, \tag{1}$$

where W represents vehicle weight, w_i represents the weight of No. i axle, and a_i and b_i are the coefficients. In this paper, the linear relation between axle weight and vehicle weight is inherited, and the coefficients of the linear relationship are estimated based on the measured vehicle data. The coefficients for different vehicle models are shown in Table 5.

3.5. Fatigue Analysis Based on Measured Vehicle Models. In order to verify the applicability of the above measured fatigue-loaded vehicle models, a representative prestressed concrete simply supported T-shaped beam bridge on the section from Kunming to Baoshan on G56 highway is selected to make the fatigue analysis. This test makes relevant fatigue analysis by means of random flow loading.

3.6. Random Traffic Simulation. Based on the above measured fatigue-loaded vehicle models, this text utilizes Monte Carlo method to make simulation of random traffic flow by means of Fortran language programming. The flow chart of random vehicle flow simulation program is shown in Figure 1.

3.7. Analysis of Fatigue Response. The above-mentioned random traffic flow simulation program is utilized to load the influence line of mid-span moment of simple supported T-shaped beam to obtain the history of load response under the

Table 4: Statistical parameters of wheelbase data.

Vehicle model	Mean value ± standard deviation of wheelbase (m)				
	Axle 1	Axle 2	Axle 3	Axle 4	Axle 5
Type 1	4.2 ± 0.936				
Type 2	4.325 ± 1.534	1.35 ± 1.773			
Type 3	3.3 ± 1.213	6 ± 2.703	1.35 ± 0.756		
Type 4	3.3 ± 1.187	1.32 ± 0.465	6 ± 2.703	1.35 ± 0.65	
Type 5	3.3 ± 1.144	1.32 ± 0.465	6 ± 2.703	1.3 ± 0.33	1.3 ± 0.335

Table 5: Parameter in a linearity fitting of axle load and vehicle weight.

Vehicle model	Fitting parameter	w_1	w_2	w_3	w_4	w_5	w_6
Type 1	a	0.23	0.77				
	b	0.58	−0.58				
Type 2	a	0.18	0.41	0.41			
	b	2.36	−1.18	−1.18			
Type 3	a	0.05	0.23	0.36	0.36		
	b	2.23	0.85	−1.54	−1.54		
Type 4	a	0.03	0.22	0.25	0.25	0.25	
	b	2.45	1.12	−1.19	−1.19	−1.19	
Type 5	a	0.03	0.14	0.14	0.23	0.23	0.23
	b	2.53	0.79	0.79	−1.37	−1.37	−1.37

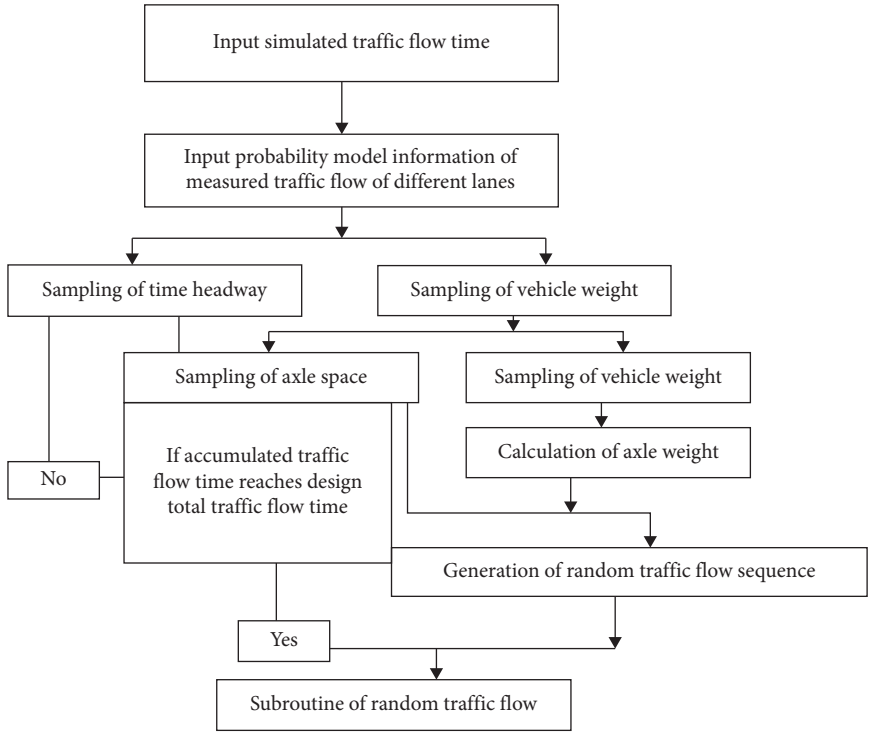

Figure 1: Flow chart of random vehicle flow simulation program.

effect 24-hour random traffic flow in Figure 2. "Drainage method" [14] is utilized to make counting statistics of the response history. Please check the statistical histogram of load amplitude distribution in Figure 3. Effective cycle index of total load amplitude is 2357 times. Response of mid-span moment of T beam under random vehicle is shown in Figure 2.

3.8. Fatigue Damage Accumulation. Fatigue load caused by random traffic flow passing through bridge belongs to variable fatigue load amplitude and is usually transformed into equivalent fatigue load amplitude for calculation [9] in the project. According to the definition, fatigue accumulating damage generated by equivalent load amplitude ΔSeq

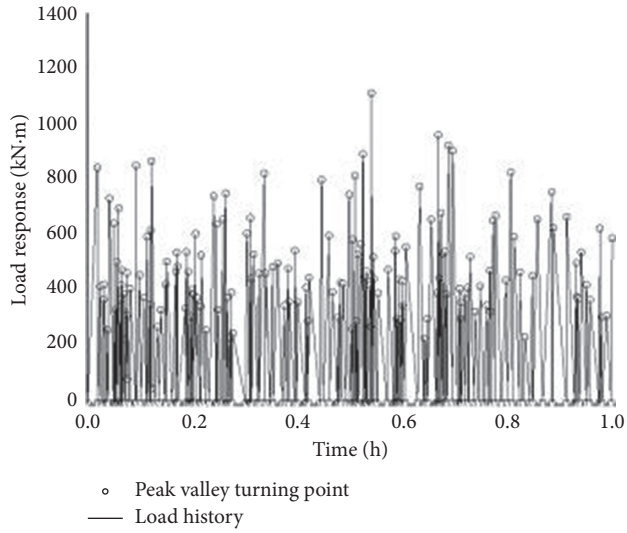

Figure 2: Response of mid-span moment of T beam under random vehicle flow.

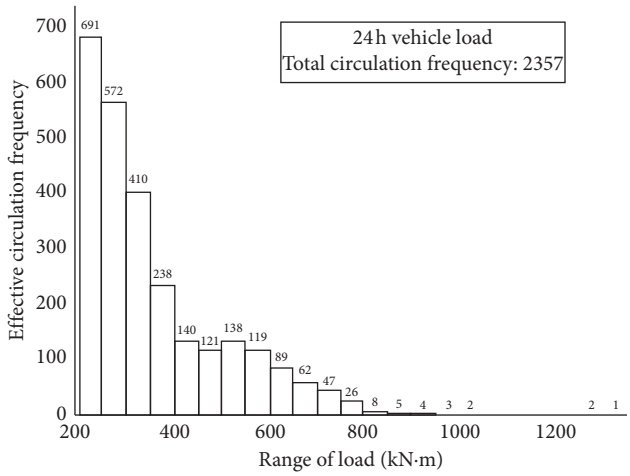

Figure 3: Statistical histogram of load amplitude distribution.

and that by variable load amplitude are equal in case of cycle indexes with the same function, which is shown below.

$$D = \sum \frac{n_i}{N_i} = \frac{\sum n_i}{N_{\text{eq}}}. \quad (2)$$

In the formula, D represents the degree of damage to component under the effect of fatigue load. That its value is 1 represents component fatigue failure. ni represents the action times of component load amplitude ΔS_i, N_i represents fatigue life of component under the effect of load amplitude ΔS_i, N_{eq} represents fatigue lift of component under the effect of equivalent load amplitude ΔS_{eq}, and $\sum n_i$ represents total action times of variable amplitude load. Approximation relation between fatigue life N and load amplitude is usually described by $N = C\Delta S^{-m}$ in component fatigue analysis and C and m are two fatigue curve parameter. If N_i and N_{eq} are represented by ΔS_{i} and ΔS_{eq}, respectively, the formula for calculating equivalent load amplitude will be as follows:

$$S_{\text{eq}} = \left(\sum \frac{n_i}{\sum n_i} \Delta S_i^m \right)^{1/m}. \quad (3)$$

In analysis of the text, load amplitude ΔS_i refers to ΔM, the mid-span moment amplitude of T-shaped beam. According to the hypothesis on force analysis of reinforced concrete structure, the equivalent stress amplitude of main tensile reinforcement in mid-span of bridge $\Delta\sigma_{\text{eq}}$ [15] is as follows:

$$\Delta\sigma_{\text{eq}} = \frac{E_s}{E_c} \frac{\Delta M_{\text{eq}} y}{I}. \quad (4)$$

In the formula, E_s and E_s are elasticity module of reinforced concrete; ΔM_{eq} is the equivalent bending moment amplitude in mid-span of T-shaped beam; y is the distance between reinforcement position and mid-span section centroid; and I is mid-span second moment of area.

With reference to *S-N* Curve put forwarded by Mason, this text makes an analysis on fatigue damage accumulation of reinforcements in concrete bridges. *S-N* Curve is as follows.

When span is over 10 m (in consideration of main reinforcement welding), the formula below is adopted for calculation.

$$\lg N = 12.7160 - 3.2599 lg\Delta\sigma. \quad (5)$$

Formulas (3)–(5) are utilized to calculate the equivalent stress amplitude of bridge reinforcements and fatigue life corresponding to effective stress amplitude. Assume that traffic flow has no obvious change within the entire design basis period. It can be calculated according to daily traffic volume and the above-mentioned fatigue life of equivalent stress amplitude that degree of fatigue damage to bridge reinforcements is 0.1045 within 100-year design basis period.

3.9. Formulation of Practical Frequency Spectrum of Fatigue Vehicle Load Model. Equivalence of each vehicle model in Table 1 is made through classic equivalence principle (equivalence of axle weight and equivalence of wheelbase) [16, 17] to transform Table 1 into practical frequency spectrum of fatigue vehicle load model for 5 vehicle models. Please check the spectrum in Table 6.

4. Determination of Standard Fatigue Vehicle

For convenience of engineering calculation, damage equivalence is made towards the above-obtained fatigue vehicle load spectrum containing 5 vehicle models to simplify it to the model of a stand fatigue vehicle. Random traffic flow simulation program that is previously compiled is slightly adjusted now to make random traffic flow become the motorcade with the same weight and wheelbase for only 1 type and to calculate the degree of fatigue damage caused by each type of fatigue vehicle model in Table 6 to mid-span concrete and reinforcement of T-shaped beam. Comparison is made between the above degree of fatigue damage and that caused by actual traffic flow in Section 3.3 to select 1 type

Table 6: Practical frequency spectrum of fatigue vehicle load model.

Vehicle model	Number of axle (piece)	Diagram	Total weight (kN)	Proportion in total traffic volume (%)
*V*1	2	40 kN 40 kN; 4.2 m	80	50.9
*V*2	3	50 kN 64 kN 64 kN; 4.325 m 1.35 m	178	5.32
*V*3	4	53 kN 60 kN 67 kN 67 kN; 3.3 m 6 m 1.35 m	247	16.07
*V*4	5	40 kN 71 kN 100 kN 73 kN 73 kN; 3.3 m 1.32 m 6 m 1.35 m	357	1.13
*V*5	6	45 kN 65 kN 90 kN 67 kN 60 kN 60 kN; 3.3 m 1.32 m 6 m 1.3 m 1.3 m	387	13

Table 7: Comparison of damage degree between different vehicles and actual traffic flow.

Vehicle model	Proportion of vehicle	*N*	Range of equivalent stress	100-year injury tolerance	Contrast percentage
*V*2	5.32%	514	21.4	0.0783	−25.0%
*V*3	16.07%	1494	15.03	0.0720	−31.1%
*V*4	1.13%	110	26	0.0316	−69.7%
*V*5	13.00%	1338	17.47	0.1052	0.1%
Actual traffic flow	—	2357	14.65	0.1045	—

Proportion of vehicle in the table represents the ratio of the quantity of this vehicle model to actual traffic flow. *N* and range of equivalent stress are both calculation results under 24 hours. Contrast percentage is the percentage of difference from the damage degree of actual traffic flow.

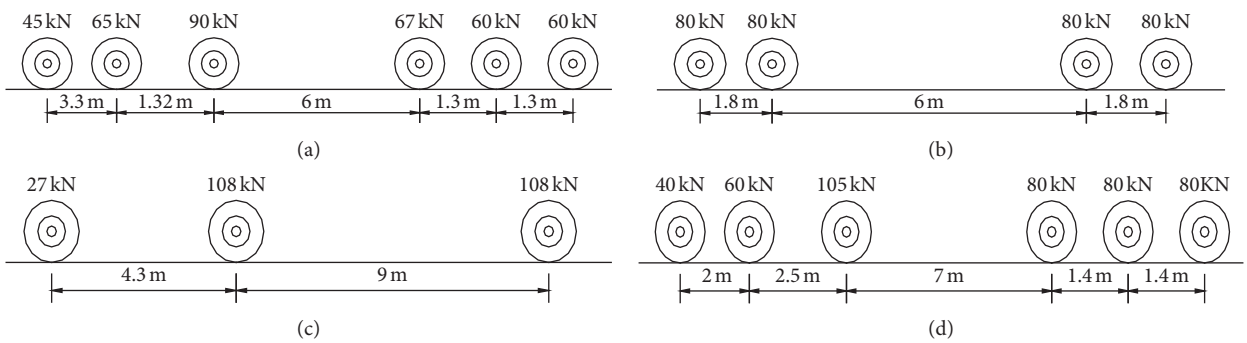

Figure 4: Standard fatigue vehicle layout. (a) Standard fatigue vehicle layout in this paper. (b) Standard fatigue vehicle layout in BS5400. (c) Standard fatigue vehicle layout in AASHTO. (d) Standard fatigue vehicle layout in General code of China.

with minimum difference in damage as standard fatigue vehicle. Comparison results are shown in Table 7.

Seen from comparison results in Table 7, damage degree under *V*5 fatigue vehicle model and damage degree caused by actual traffic flow have minimum deviation so *V*5 is regarded as standard fatigue vehicle whose specific arrangement is shown in Figure 4(a). At the same time, Figure 4 also gives specific arrangement for standard fatigue vehicles in different specifications. "General Code" in the figure identifies General Code for Design of Highway Bridges and Culverts. Standard fatigue vehicle layout is shown in Figure 4.

Each standard vehicle is loaded to the influence line of T-shaped beam through traffic flow program and its degree of fatigue damage is calculated. Calculation result and degree of fatigue damage caused by actual traffic flow to T-shaped beam are compared and comparison results are shown in Table 8.

Table 8: Comparison of fatigue damage caused by different standard fatigue vehicles.

	Proportion of vehicle	N	Range of equivalent stress	100-year injury tolerance	Contrast percentage
Traffic flow	13%	2357	14.650	0.1045	—
"General Code"	13%	1339	20.340	0.1730	65.53%
BS5400	13%	1337	18.998	0.1383	32.35%
AASHTO	13%	1333	16.095	0.0832	−20.41%
This text	13%	1338	17.472	0.1052	0.66%

Proportion of vehicle in the table represents the ratio of the quantity of this vehicle model to actual traffic flow. N and range of equivalent stress are both calculation results under 24 hours. Contrast percentage is the percentage of difference from the damage degree of actual traffic flow.

As Seen from Table 8, standard fatigue vehicles mentioned in "General Code" and BS5400 Specification both overestimate the fatigue damage to bridges in Yunnan Province caused by actual traffic on highways, but AASHTO Specification underestimates the fatigue damage to bridge. However, standard vehicle raised in this text is relatively closer to the fatigue damage to bridges in Yunnan Province caused by actual traffic on highways. Thus, standard vehicle raised in this text is more applicable to the fatigue design of highway bridges in Yunnan Province.

5. Conclusion

This paper makes an investigation and analysis on the traffic volume of G56 highway in Yunnan Province. Wireless sensors network is used to collect traffic flow data on the highway. The data collected by the wireless sensor layer is analyzed to realize local short-term storage of monitoring data and then effective processing of the data. Based on the investigation of the most representative expressway traffic flow, the clustering method is applied to classify the vehicle models. In addition, the weight probability distribution model of different vehicle models is developed through statistical analysis, which simplifies the fatigue intensity spectrum model of composition. It was observed that the selection of five vehicles of equivalent model followed by six-axle vehicle has the greatest impact on bridge fatigue damage as the standard fatigue vehicle. The research results provided a basis for the fatigue design of highway bridges in plateau and mountainous areas and provided data for the development of vehicle fatigue load spectra in national highway regions.

Data Availability

The analysis data are included in the manuscript.

Conflicts of Interest

The authors declare that there are no conflicts of interest regarding the publication of this paper.

Acknowledgments

This work was financially supported by the National Natural Science Foundation of China (No. 51568029).

References

[1] AASHTO LRFD, *Bridge Design Specifications*pp. 14–36, Texas Department of Transportation, Austin, TX, USA, 6th edition, 2012.

[2] CCCC Highway Consultants Co., Ltd., "JTG D60-2015," *General Specifications for Design of Highway Bridges and Culverts*, pp. 115–126, China Communication Press, Beijing, China, 2016.

[3] C.-H. Chen, F. Song, F.-J. Hwang, and L. Wu, "A probability density function generator based on neural networks," *Physica A: Statistical Mechanics and Its Applications*, vol. 541, Article ID 123344, 2020.

[4] Y. H. Shao and P. M. Lv, "Fatigue load spectrum for Jiujiang Yangtze River bridge," *Journal of Chang'an University: Natural Science Edition*, vol. 35, no. 5, pp. 50–56, 2015.

[5] T. Y. Jiang, "Investigation on the random vehicle load spectrum of the highway," *Bridge Journal of Changsha University of Science and Technology: Natural Science*, vol. 12, no. 3, pp. 56–62, 2015.

[6] C. Wang, "Study on load spectrum and fatigue performance of the fatigue vehicle in the small-span PC girder bridge on heavy-load highway," pp. 12–16, Beijing Jiaotong University, Beijing, China, 2015, Master's Thesis.

[7] B. Chen, X. Li, X. Xie, Z. Zhong, and P. Lu, "Fatigue performance assessment of composite arch bridge suspenders based on actual vehicle loads," *Shock and Vibration*, vol. 2015, no. 5, 13 pages, Article ID 659092, 2015.

[8] J. F. Zhao, "Study on loads of regular vehicles and extra heavy vehicles on multi regional highway bridges," pp. 3–11, Chang'an University, Xi'an, China, 2014, Master's Thesis.

[9] R. Li, "Study on joint fatigue life of concrete filled steel tubular truss arch bridge," pp. 37–49, Kunming University of Science and Technology, Kunming, China, 2012, Doctor's Thesis.

[10] H. Wang, Q. Chen, and Y. Zhang, "On the LLR criterion based shortening design for LDPC codes," in *Proceedings of the IEEE 2016 Annual Conference on Information Science and Systems*, Princeton, NJ, USA, March 2016.

[11] A. Wongsriwor, V. Imtawil, and P. Suttisopapan, "Design of rate-compatible LDPC codes based on uniform shortening distribution," *Engineering and Applied Science Research*, vol. 45, no. 2, pp. 140–146, 2018.

[12] M. Baldi, N. Maturo, E. Paolini, and F. Chiaraluce, "On the use of ordered statistics decoders for low-density parity-check codes in space telecommand links," *EURASIP Journal on Wireless Communications and Networking*, vol. 6, p. 272, 2016.

[13] M. Beermann, T. Breddermann, and P. Vary, "Rate-compatible LDPC codes using optimized dummy bit insertion," in *Proceedings of the 8th International Symposium on Wireless Communication Systems*, pp. 447–451, Aachen, Germany, November 2011.

[14] CCSDS, "Short block length LDPC codes for TC synchronization and channel coding," *Orange Book. CCSDS*, vol. 231, 2015.

[15] W. Sun, S. Yu, W. Lou, Y. T. Hou, and H. Li, "Protecting your right: verifiable attribute-based keyword search with fine-grained owner-enforced search authorization in the cloud,"

IEEE Transactions on Parallel and Distributed Systems, vol. 27, no. 4, pp. 1187–1198, 2016.

[16] Y. Miao, J. Ma, X. Liu, J. Weng, H. Li, and H. Li, "Lightweight fine-grained search over encrypted data in fog computing," *IEEE Transactions on Services Computing*, vol. 12, no. 5, pp. 772–785, 2019.

[17] M. Ibrar, A. Akbar, R. Jan et al., "ARTNet: AI-based resource allocation and task offloading in a reconfigurable internet of vehicular networks," *IEEE Transactions on Network Science and Engineering*, vol. 7, 2020.